NASA/TM—2015-218731

Mechanical Properties of Graphene Nanoplatelet/ Carbon Fiber/Epoxy Hybrid Composites: Multiscale Modeling and Experiments

C.M. Hadden and D.R. Klimek-McDonald
Michigan Technological University, Houghton, Michigan

E.J. Pineda
Glenn Research Center, Cleveland, Ohio

J.A. King, A.M. Reichanadter, I. Miskioglu, S. Gowtham, and G.M. Odegard
Michigan Technological University, Houghton, Michigan

June 2015

NASA STI Program . . . in Profile

Since its founding, NASA has been dedicated to the advancement of aeronautics and space science. The NASA Scientific and Technical Information (STI) Program plays a key part in helping NASA maintain this important role.

The NASA STI Program operates under the auspices of the Agency Chief Information Officer. It collects, organizes, provides for archiving, and disseminates NASA's STI. The NASA STI Program provides access to the NASA Technical Report Server—Registered (NTRS Reg) and NASA Technical Report Server—Public (NTRS) thus providing one of the largest collections of aeronautical and space science STI in the world. Results are published in both non-NASA channels and by NASA in the NASA STI Report Series, which includes the following report types:

- TECHNICAL PUBLICATION. Reports of completed research or a major significant phase of research that present the results of NASA programs and include extensive data or theoretical analysis. Includes compilations of significant scientific and technical data and information deemed to be of continuing reference value. NASA counter-part of peer-reviewed formal professional papers, but has less stringent limitations on manuscript length and extent of graphic presentations.

- TECHNICAL MEMORANDUM. Scientific and technical findings that are preliminary or of specialized interest, e.g., "quick-release" reports, working papers, and bibliographies that contain minimal annotation. Does not contain extensive analysis.

- CONTRACTOR REPORT. Scientific and technical findings by NASA-sponsored contractors and grantees.

- CONFERENCE PUBLICATION. Collected papers from scientific and technical conferences, symposia, seminars, or other meetings sponsored or co-sponsored by NASA.

- SPECIAL PUBLICATION. Scientific, technical, or historical information from NASA programs, projects, and missions, often concerned with subjects having substantial public interest.

- TECHNICAL TRANSLATION. English-language translations of foreign scientific and technical material pertinent to NASA's mission.

For more information about the NASA STI program, see the following:

- Access the NASA STI program home page at http://www.sti.nasa.gov

- E-mail your question to help@sti.nasa.gov

- Fax your question to the NASA STI Information Desk at 757-864-6500

- Telephone the NASA STI Information Desk at 757-864-9658

- Write to:
  NASA STI Program
  Mail Stop 148
  NASA Langley Research Center
  Hampton, VA 23681-2199

NASA/TM—2015-218731

Mechanical Properties of Graphene Nanoplatelet/ Carbon Fiber/Epoxy Hybrid Composites: Multiscale Modeling and Experiments

C.M. Hadden and D.R. Klimek-McDonald
Michigan Technological University, Houghton, Michigan

E.J. Pineda
Glenn Research Center, Cleveland, Ohio

J.A. King, A.M. Reichanadter, I. Miskioglu, S. Gowtham, and G.M. Odegard
Michigan Technological University, Houghton, Michigan

Prepared for the
20th International Conference on Composite Materials
cosponsored by Siemens, LM Wind Power, GOM, Zebicon, Force Technology, et al.
Copenhagen, Denmark, July 19–24, 2015

National Aeronautics and
Space Administration

Glenn Research Center
Cleveland, Ohio 44135

June 2015

Acknowledgments

This research was funded by NASA under the Aeronautical Sciences Program (Grant NNX11A072A), the Air Force Office of Scientific Research under the Low Density Materials Program (Grant FA9550-13-1-0030), the Michigan Space Grant Consortium (Grant 2993583), the NSF I/UCRC on Novel High Voltage/Temperature Materials and Structures (Grant IIP-1362040), and the Michigan Technological University Summer Undergraduate Research Fellowship Program. The authors thank XG Sciences for donating graphene nanoplatelets and Hexcel for donating AS4 carbon fiber for this work. The authors would also like to thank the following undergraduate students for their assistance on this project: Michael T. Best, Courtney A. Castelic, James A. Kenney, Kerry L. King, Andrew P. Lewis, Ryan E. McInnis, Mary Kate Mitchell, Ryan J. Patrick, Andrew N. Payton, Travis J. D. Pellosma, Alexander E. Powell, Elizabeth J. Skultety, Stephanie L.Tankersley, Peter H. Winegar, and Lucas D. Zoromski. SUPERIOR, a high-performance computing cluster at Michigan Technological University, was used in obtaining results presented in this publication.

Level of Review: This material has been technically reviewed by technical management.

Available from

NASA STI Program
Mail Stop 148
NASA Langley Research Center
Hampton, VA 23681-2199

National Technical Information Service
5285 Port Royal Road
Springfield, VA 22161
703-605-6000

This report is available in electronic form at http://www.sti.nasa.gov/ and http://ntrs.nasa.gov/

Mechanical Properties of Graphene Nanoplatelet/Carbon Fiber/Epoxy Hybrid Composites: Multiscale Modeling and Experiments

C.M. Hadden and D.R. Klimek-McDonald
Michigan Technological University
Houghton, Michigan 49931

E.J. Pineda
National Aeronautics and Space Administration
Glenn Research Center
Cleveland, Ohio 44135

J.A. King, A.M. Reichanadter, I. Miskioglu, S. Gowtham, and G.M. Odegard
Michigan Technological University
Houghton, Michigan 49931

Abstract

Because of the relatively high specific mechanical properties of carbon fiber/epoxy composite materials, they are often used as structural components in aerospace applications. Graphene nanoplatelets (GNPs) can be added to the epoxy matrix to improve the overall mechanical properties of the composite. The resulting GNP/carbon fiber/epoxy hybrid composites have been studied using multiscale modeling to determine the influence of GNP volume fraction, epoxy crosslink density, and GNP dispersion on the mechanical performance. The hierarchical multiscale modeling approach developed herein includes Molecular Dynamics (MD) and micromechanical modeling, and it is validated with experimental testing of the same hybrid composite material system. The results indicate that the multiscale modeling approach is accurate and provides physical insight into the composite mechanical behavior. Also, the results quantify the substantial impact of GNP volume fraction and dispersion on the transverse mechanical properties of the hybrid composite while the effect on the axial properties is shown to be insignificant.

1.0 Introduction

Carbon/epoxy composites are a prime component of many modern aircraft structures because of their exceptional mechanical properties relative to their bulk mass density. The bulk-level mechanical properties of these composites depend directly on the mechanical properties and interaction between the constituent materials. Traditionally, the constituents have been carbon fibers and epoxy matrix. However, the inclusion of graphene nanoplatelets (GNPs) in epoxy has been shown to improve mechanical and electrical properties with respect to the un-reinforced epoxy (Refs. 1 to 4), thus showing promise for use of GNP-reinforced epoxy as the matrix phase in a fiber composite. The resulting GNP/carbon fiber/epoxy hybrid composite could potentially show improvements in mechanical properties with respect to traditional carbon fiber/epoxy composites.

It has been demonstrated (Refs. 2 to 4) that the effect of GNPs on GNP/polymer composite mechanical properties is governed by the amount of GNPs added to the polymer and the dispersion of the GNPs within the polymer. It has been also shown through experimentally-validated molecular modeling (Ref. 5) that the GNP/epoxy interface contains an interphase region that is on the same size order as GNP sheets and can be sensitive to epoxy crosslink density. The interphase region is composed of epoxy molecules that have a mass density that is significantly different than that of the bulk. However, it is uncertain how the molecular structure of the interphase region and molecular-scale dispersion of GNPs

affects the bulk-level elastic properties of GNP/carbon fiber/epoxy hybrid composites. Molecular modeling must be used to provide a sufficient amount of physical insight into the effect of the interphase molecular structure and the dispersion of GNPs on bulk-level performance of the hybrid composite because of the difficulty in experimentally characterizing these factors.

The objective of this study is to use an experimentally validated multiscale modeling technique to determine the molecular structure of the GNP/epoxy interface and understand the influence of the interface, GNP dispersion, and GNP volume fraction on the bulk-level elastic properties of a GNP/carbon fiber/epoxy hybrid composite. The multiscale modeling approach consists of molecular dynamics (MD) and micromechanics modeling. The multiscale model is validated by direct comparison to mechanical properties of the hybrid composite determined by mechanical testing of fabricated specimens. The results indicate that the multiscale model accurately predicts the bulk-level mechanical properties based on molecular-level structure, and GNP dispersion has a tremendous effect on the hybrid composite response.

2.0 Multiscale Modeling

MD was used to predict the molecular structure and elastic properties of a representative volume element (RVE) containing GNP and the GNP/epoxy interphase region. The corresponding homogenized elastic properties, including the influence of the interphase region, were used in subsequent, uncoupled, micromechanical analyses to predict the mechanical response of the GNP/epoxy composite as well as the GNP/carbon fiber/epoxy hybrid composite. The details of the multiscale modeling are given in this section. The modeled epoxy system consisted of the EPON 862 (diglycidyl ether of bisphenol F, DGEBF) monomer and the EPIKURE Curing Agent W (diethyltoluenediamine, DETDA).

2.1 MD Modeling

MD techniques have been used in several instances to model pure thermoset EPON 862/DETDA epoxy systems (Refs. 6 to 9). MD modeling has also been performed on thermoset polymers containing carbon nanotubes (Refs. 10 to 17), nanoparticles (Refs. 18 to 20), and in the presence of a surface (Refs. 5, 21 to 24). The interfacial region between epoxy and carbon reinforcement (either carbon fiber or GNP) has been investigated in many of the aforementioned references. These MD studies, coupled with recent backing from experimental imagery (Ref. 5), have revealed the existence of an interfacial region near the carbon reinforcement surface in which the local epoxy molecular structure, specifically the mass density, differs from that of the bulk. For the GNP-reinforced EPON 862/DETDA system, previous research has shown this interfacial region to be approximately 10 Å thick from the graphite surface (Ref. 5). Although these studies have given valuable information regarding the physical nature of the interfacial region, there has been little effort to implement this information into a bulk-scale model for GNP/epoxy composites.

The MD model of the GNP/epoxy interface was constructed using a multistep approach. First, a model of the pure uncrosslinked epoxy system was established. Second, a series of GNP sheets was added to the model of the pure epoxy system to establish the GNP/epoxy interface model for different numbers of GNP sheets. Finally, the GNP/epoxy MD models were crosslinked to various levels. Each of these steps is described in the following subsections. After the systems were constructed, they were exposed to applied deformations to predict their mechanical response. The Large Scale Atomic/Molecular Massively Parrallel Simulator (LAMMPS) software package (Ref. 25) was used for all of the Molecular Minimization (MM) and MD simulations described herein.

2.1.1 Pure Epoxy MD Model

The initial uncrosslinked polymer molecular structure was established using a procedure similar to that of Bandyopadhyay et al. (Ref. 6), consisting of the EPON 862 monomer and the DETDA hardener shown in Figure 1. A stoichiometric mixture of 2 molecules of EPON 862 and 1 molecule of DETDA was placed in a MD simulation box with periodic boundary conditions. The initial atomic coordinates file was

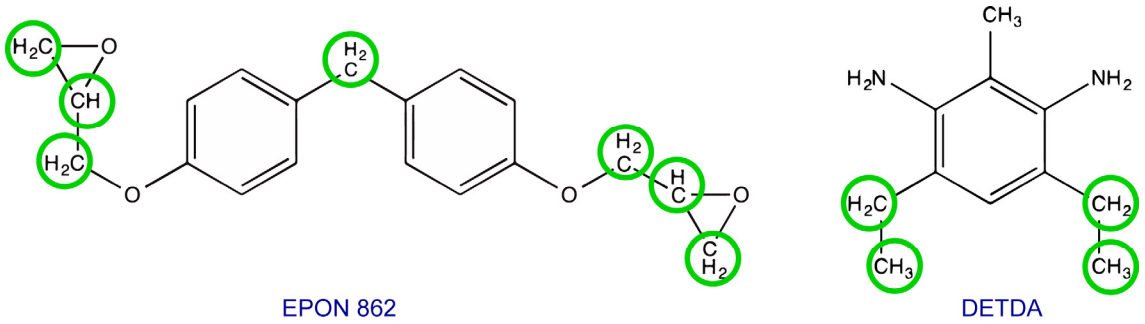

Figure 1.—Molecular structures of EPON 862 and DETDA. Green circles indicate united atoms.

written in the native LAMMPS format and the Optimized Potential for Liquid Simulations (OPLS) United Atom force field developed by Jorgensen and co-workers (Refs. 26 and 27) was used for defining the bond, angle, and dihedral parameters. The equilibrium spacing parameter σ of the Lennard-Jones potential was taken to be the arithmetic mean of the individual parameters of the respective atom types, while the well-depth parameter ε was taken to be the geometric mean of the values for the respective atom types. The van der Waals interactions were modeled with an interaction cutoff radius of 10Å.

This particular force field allows for modeling of CH_3, CH_2, CH, and alkyl groups as single united atoms with their corresponding masses. The described polymer model utilized united atom structures for all applicable groups, except for the C and H atoms in the phenyl rings for both monomer and hardener molecules along with one CH_3 group directly connected to the phenyl ring of the DETDA molecule. Thus, the use of united atoms reduced the modeled 2:1 structure from 117 to 83 atoms. The location of each united atom is shown in Figure 1, with 31 total atoms in the molecule of EPON 862 and 21 in the molecule of DETDA.

The 2:1 molecular model was subjected to four MM minimizations and three 100 ps MD simulations. MM simulations utilized the conjugate gradient stopping criterion, and MD simulations were performed using the NVT (constant volume and temperature) ensemble at 300 K. This process minimized internal forces and thus reduced internal residual stresses that were created from the initial construction of bonds, bond angles, and bond dihedrals.

2.1.2 Epoxy/GNP Model

After the structure stabilized to a relatively low energy value, the initial 2:1 stoichiometric structure was replicated, and the replicated models were randomly rotated and then translated along the three Cartesian axes and combined into a much larger structure with an EPON 862:DETDA ratio of 250:125, containing 10,375 total united atoms. Therefore, the resulting system consisted of 250 randomly oriented clusters of the small 2:1 ratio cluster stacked loosely together in a manner much like that of a simple cubic crystal structure.

This larger polymer model was mirrored about a graphene structure positioned in the *x*-*y* plane central to the *z*-axis (Fig. 2). As a result, each system contains a 500:250 ratio of EPON 862:DETDA totaling 20,750 polymer atoms. The centralized graphene structures varied in thickness from 1 atomic layer to 4 layers thick, each layer containing 4200 carbon atoms. The largest system, comprised of a 4-layer graphene sheet, contained 37,550 total atoms and the initial box size was 101×104×210 Å. All models employed 3-D periodic boundary conditions. The initial box size produced a polymer density approximately equal to half of a fully cured solid EPON 862 epoxy (~0.5 g/cc in all four systems).

In order to achieve the desired polymer density of 1.17 g/cc, the four separate models were subjected to twelve cycles of deformation along the *z*-axis (Fig. 2). Each cycle included a MM followed by a 100 ps MD NVT simulation in which the *z* coordinate was reduced in equal amounts from both the positive and negative *z*-coordinate boundaries using the LAMMPS fix/deform tool. A Nose/Hoover thermostat and barostat was implemented for temperature and pressure control, respectively (Ref. 28). The amount of deformation decreased with each cycle as the models became closer to the desired density. This was done

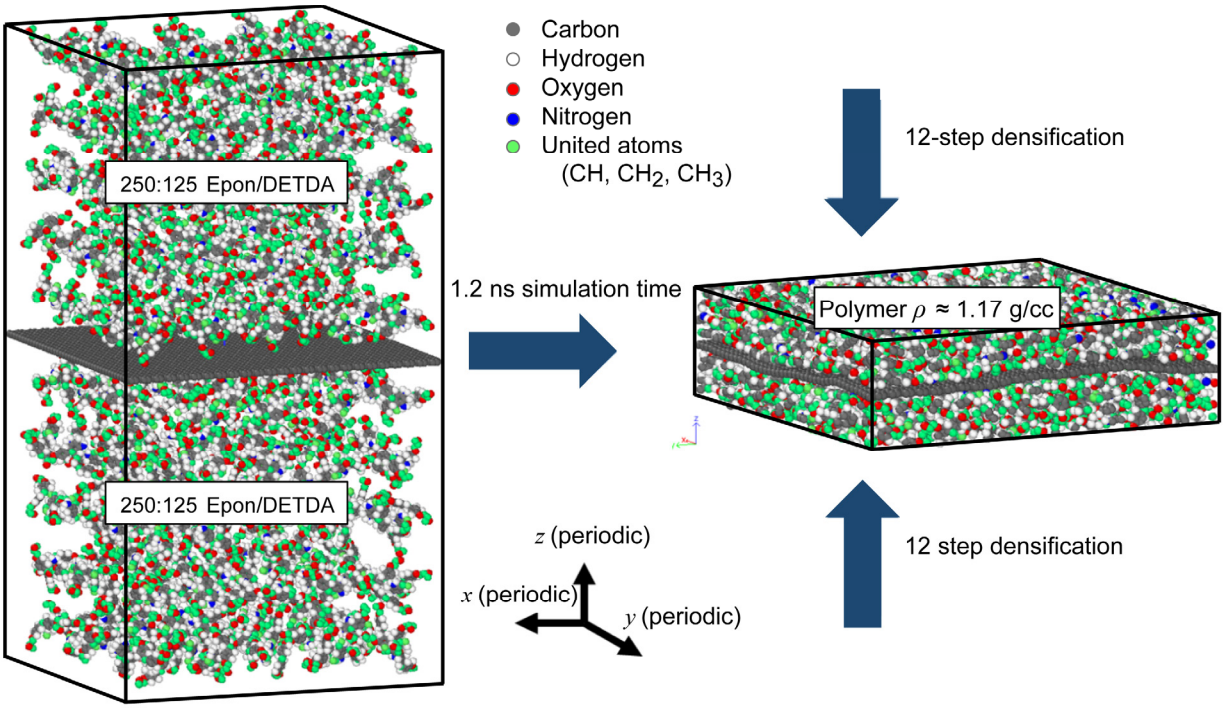

Figure 2.—Molecular structures for a single graphene sheet system highlighting the densification process.

to avoid large energy increases to the system by packing the molecules together too quickly. This entire densification process was performed over a total of 1.2 ns for each of the four systems. The final *z*-coordinate boundary enabled for polymer atoms to extend ~13 Å from the graphene surface, to ensure that the interfacial region was fully captured and to show a minimal influence from the bulk polymer characteristics during deformation. The fully equilibrated, noncrosslinked, structures for all four systems are shown in Figure 3.

2.1.3 Crosslinking Procedure

The equilibrated models were crosslinked based on the root mean square (RMS) distance between the CH_2 groups of the EPON 862 and the N atoms of DETDA molecules using the same procedure described previously (Ref. 5). A total of 16 molecular systems were established, each having a unique crosslink density (65, 70, 75, and 80 percent) and number of graphene layers (1-4). The crosslink density was defined as the ratio of the total number of crosslinks that were formed to the maximum number of crosslinks that could be formed. It is important to note that for industrial grade epoxies, a broad range of crosslink densities of 60 to 95 percent is typically observed in experiments (Refs. 29 to 33). Therefore, the simulated crosslink densities were chosen to span part of this range. It was observed that crosslinking above 80 percent resulted in molecular structures with unnaturally high internal stresses.

After crosslinking to the desired density, each structure was allowed to equilibrate using a series of three MM minimizations and two MD NVT simulations of 2 ns each. A 1 ns NPT (constant pressure and temperature) simulation followed to minimize internal stresses. The density of formed crosslink atoms (C-N and O-H) as a function of the *z*-axis is shown in Figure 4, where the origin of the *z*-axis lies in the center of the graphene structures and the mass density is calculated for all values of *x* and *y*. The figure contains data for 80 percent crosslinked structures only, and shows good dispersion of crosslinks throughout the polymer structure with unique profiles for each crosslink density. Crosslink density profiles for 65, 70, and 75 percent crosslinked structures were similar.

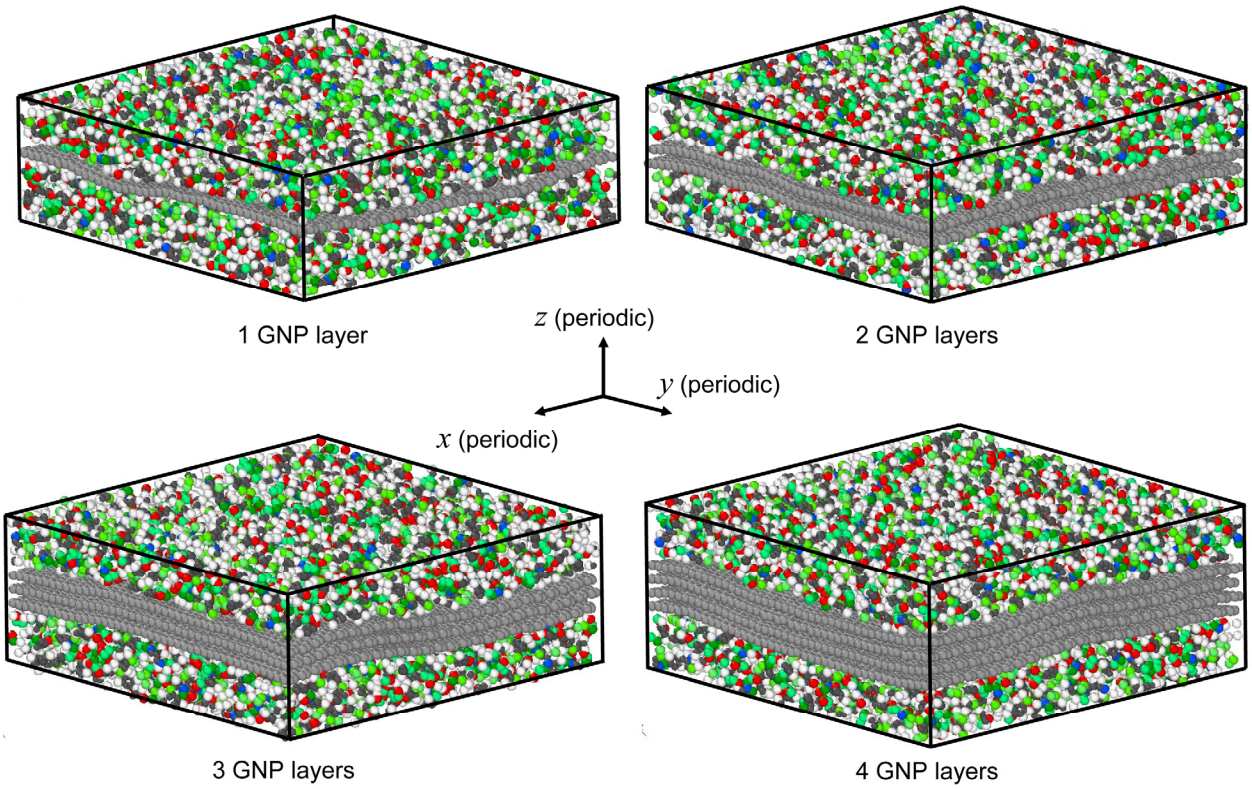

Figure 3.—Equilibrated models for varying number of graphene layers before crosslinking. Average polymer density ~1.17 g/cc for each model.

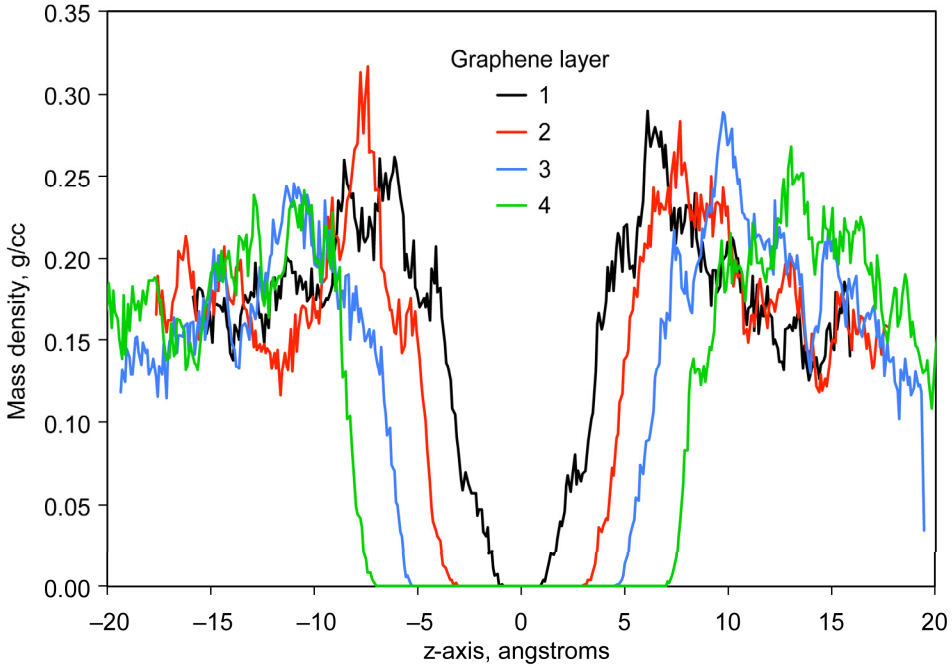

Figure 4.—Mass density profile of crosslinked atoms as a function of z-axis coordinate for 80 percent crosslinked systems. The center of the MD model corresponds to z = 0.

Shown in Figures 5 to 8 is the overall mass density of the 16 models along the *z*-axis, which were calculated the same way as with Figure 4. These curves follow a similar trend to that demonstrated by Hadden et al. (Ref. 5). There are large peaks at the locations corresponding to the graphene sheets. These peaks are not perfectly symmetrical because the equilibrium configuration of the graphene sheets includes a considerable amount of waviness (Fig. 3). Immediately adjacent to these peaks are smaller peak values of density of epoxy near the graphene surface, followed by diminishing oscillations along the *z*-axis. At about ~10 Å from the outer graphene surfaces the density is steady near the bulk density level of 1.17 g/cc, thus the interphase region is ~10 Å thick.

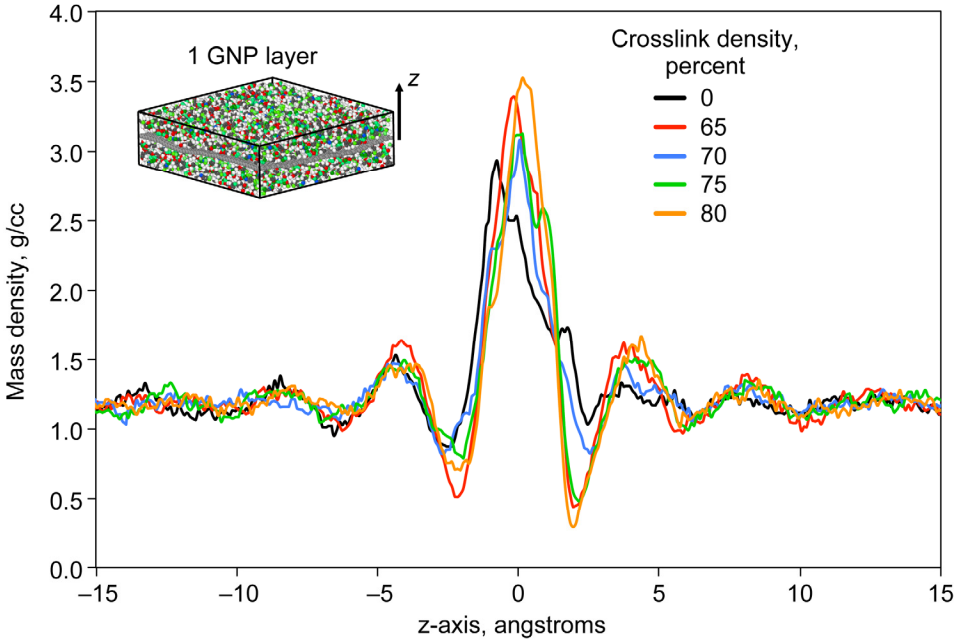

Figure 5.—Atomic mass density profile along z-axis for 1 layer of graphene.

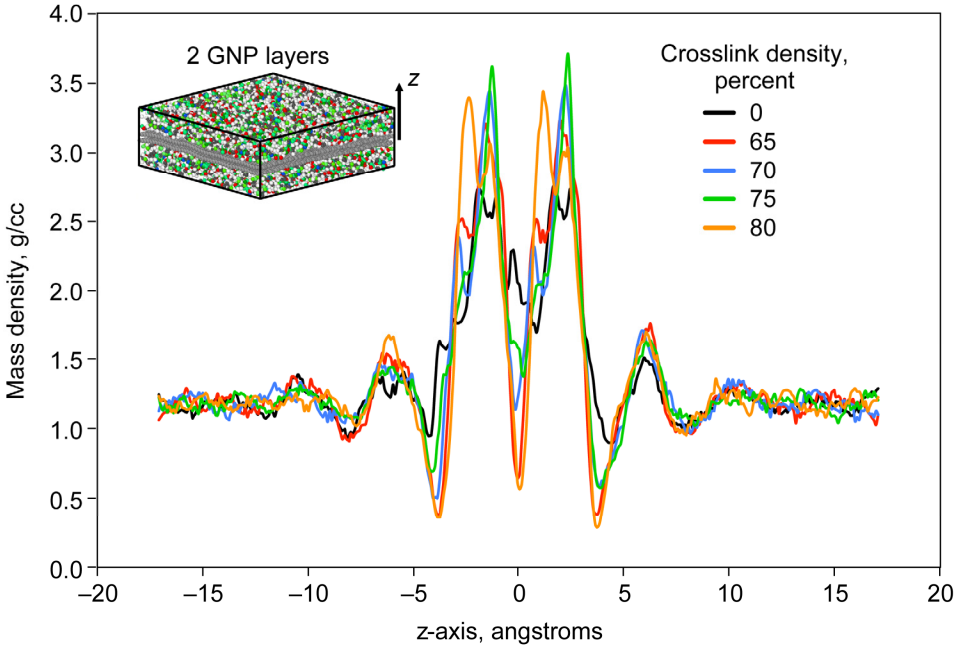

Figure 6.—Atomic mass density profile along z-axis for 2 layers of graphene.

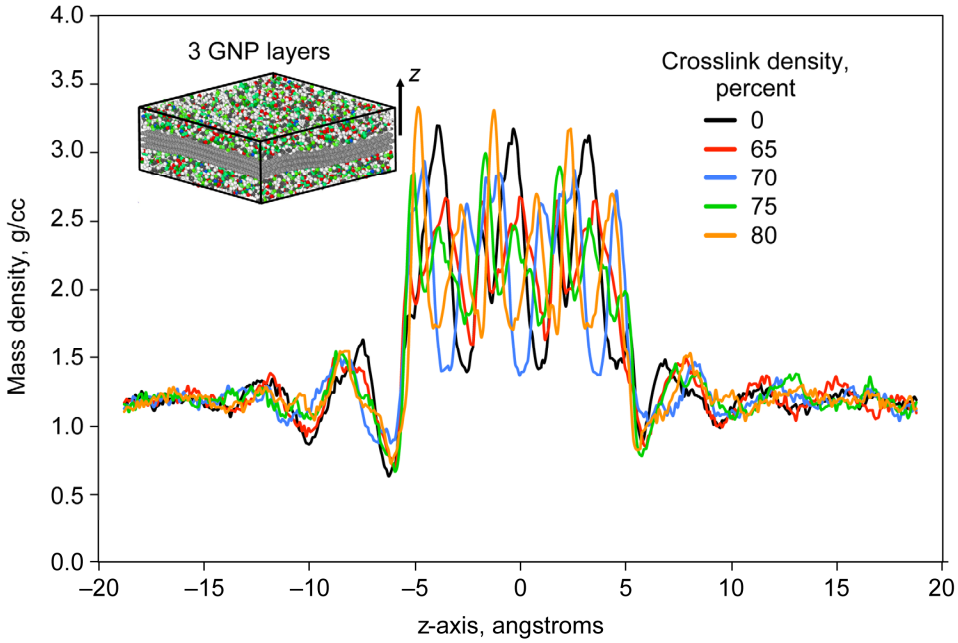

Figure 7.—Atomic mass density profile along z-axis for 3 layers of graphene.

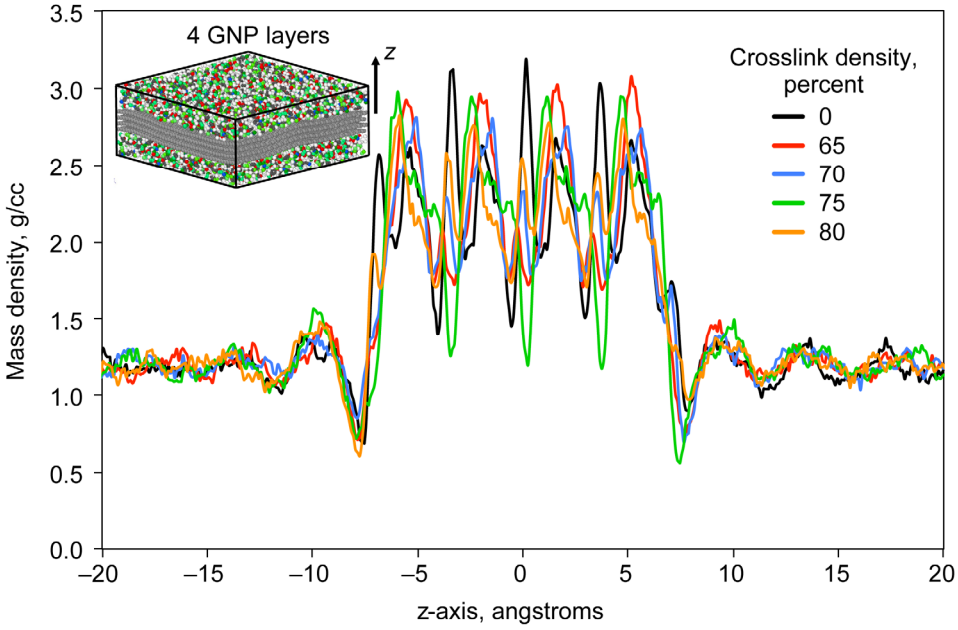

Figure 8.—Atomic mass density profile along z-axis for 4 layers of graphene.

2.1.4 Mechanical Deformation

The 16 molecular models were subjected to MD-simulated uniaxial mechanical deformations to predict their elastic mechanical responses. The models were deformed with uniaxial 5 percent strains in tension and compression along the *x*-, *y*-, and *z*-axes over a period of 1 ns. Poisson contractions were allowed in the transverse directions for the direct calculation of Young's modulus and Poisson's ratio. Additionally, shear deformations of 5 percent were performed separately along the *x*-*y*, *y*-*z*, and *x*-*z* planes over the period of 1 ns for each model. Representative stress versus strain curves for the tensile deformation along the *x*-axis and shear in the *x*-*y* plane are shown for the 80 percent crosslinked models in Figure 9. The corresponding stress-strain behavior for the other crosslink densities and deformation modes showed similar trends. The values of Young's modulus in the three orthogonal directions (E_x, E_y, E_z), the shear modulus in the *x*-*y* plane (G_{xy}), and the Poisson's ratios for all 16 systems are given in Table 1. The shear modulus values in the *y*-*z* and *x*-*z* planes are not included in Table 1 because they were nearly zero-valued based on the dominance of the van der Waals bonds between the graphene sheets and polymer and the periodic boundary conditions. As expected, the values of E_z are much lower than those of E_x and E_y because the dominance of van der Waals forces in that direction and because the graphene is alined in the *x*-*y* plane. The volume fraction of the graphene (v_{GNP}) for each of the 16 MD models is also given in Table 1.

From Figure 9 it is clear that there was a linear-elastic response of the models up to tensile and shear strains of 5 percent. From Table 1 it can be seen that E_x and E_y are nearly identical in each model, as is expected given the material symmetry (Fig. 3). E_z was much lower in magnitude than E_x and E_y because the graphene sheets were oriented in the *x*-*y* plane. The overall magnitude of E_x, E_y, and G_{xy} increase substantially with the number of graphene layers, which corresponds to the increase of v_{GNP}. The values of Poisson's ratio do not appear to be strongly dependent on the number of graphene layers in the model. There appears to be no significant influence of the epoxy crosslink density on the elastic properties of the interface.

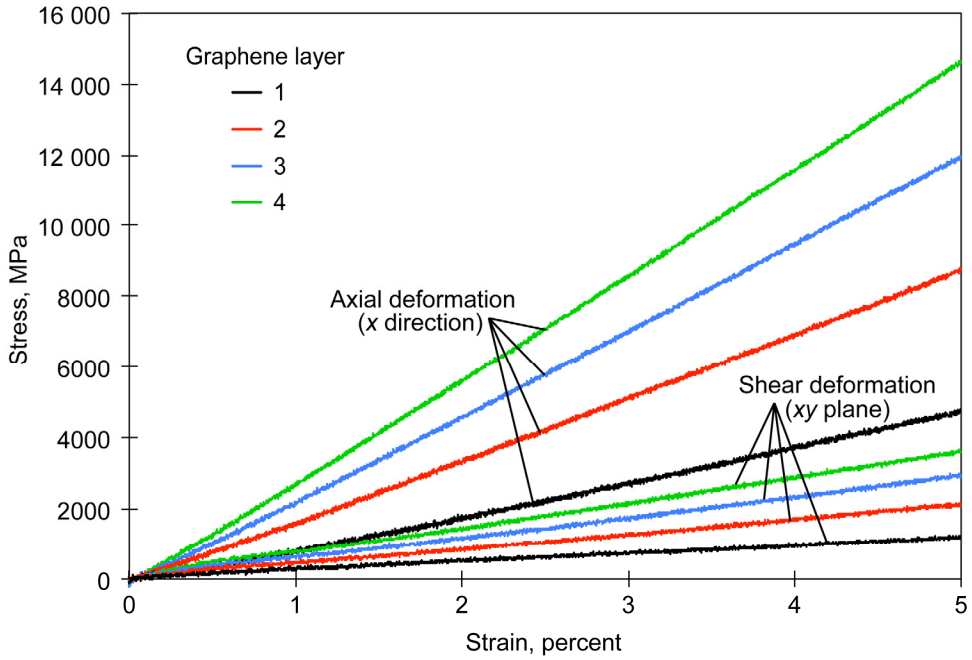

Figure 9.—Representative axial and shear stress versus strain curves for 80 percent crosslinked structures.

TABLE 1.—PREDICTED ELASTIC PROPERTIES FROM MD SIMULATIONS (MODULUS GIVEN IN GPa)

Epoxy crosslink density, percent	v_{GNP}	E_x	E_y	E_z	G_{xy}	v_{xy}	v_{yx}	v_{xz}	v_{yz}	v_{zx}	v_{zy}
65	1 layer—0.111	94.0	94.2	2.397	0.242	0.132	0.148	0.636	0.590	0.018	0.004
65	2 layers—0.187	177.4	175.7	2.846	0.433	0.153	0.152	0.615	0.584	0.012	0.071
65	3 layers—0.271	240.5	238.1	2.855	0.580	0.155	0.150	0.490	0.479	0.002	0.033
65	4 layers—0.330	294.4	291.9	3.218	0.705	0.153	0.153	0.489	0.501	0.007	0.073
70	1 layer—0.111	93.3	93.0	2.590	0.290	0.142	0.146	0.491	0.500	0.042	0.083
70	2 layers—0.187	170.4	170.7	3.008	0.424	0.146	0.159	0.468	0.462	0.042	0.007
70	3 layers—0.271	240.0	236.8	2.815	0.483	0.153	0.151	0.500	0.490	0.010	0.023
70	4 layers—0.330	294.5	295.3	3.294	0.542	0.153	0.155	0.507	0.454	0.011	0.035
75	1 layer—0.111	91.9	93.8	2.684	0.234	0.144	0.157	0.516	0.564	0.095	0.049
75	2 layers—0.187	174.8	175.2	2.768	0.429	0.154	0.163	0.550	0.516	0.017	0.018
75	3 layers—0.271	238.6	238.1	3.034	0.579	0.154	0.151	0.514	0.493	0.020	0.004
75	4 layers—0.330	293.5	293.4	3.244	0.713	0.163	0.154	0.483	0.535	0.007	0.010
80	1 layer—0.111	93.4	94.8	2.432	0.243	0.130	0.158	0.460	0.471	0.109	0.025
80	2 layers—0.187	174.6	172.5	2.731	0.424	0.168	0.153	0.437	0.524	0.056	0.015
80	3 layers—0.271	239.4	238.3	3.005	0.582	0.152	0.151	0.440	0.446	0.010	0.034
80	4 layers—0.330	293.1	295.5	3.251	0.725	0.159	0.156	0.455	0.452	0.011	0.009

2.2 Micromechanics

Once the mechanical response of the molecular models shown in Figure 3 was determined, then the elastic properties shown in Table 1 were used as input to the next higher length-scale (continuum) analysis. Figure 10 shows the modeling strategy for using the molecular-scale elastic properties for ultimately predicting the elastic properties of the GNP/carbon fiber/epoxy hybrid composite.

The generalized method of cells (GMC) micromechanics theory was used to provide the continuum-level predictions (Refs. 34 to 36). With this method, a repeating unit cell (RUC) representing the periodic material microstructure is devised. This RUC may contain as many constituent phases as is necessary to represent the composite material accurately. The RUC is discretized into a number of subcells, each of which is occupied by a single phase of the composite. Continuity of displacement and traction is enforced at each of the subcell interfaces, along with periodic boundary conditions, in an average (or integral) sense, to arrive at a strain concentration matrix. Once the strain concentration matrix is obtained, the local subcell stresses and strains, and the homogenized RUC stiffness tensor, can be readily obtained. The semi-analytical procedure is extremely computationally efficient and provides solutions on the order of seconds, or less.

GMC is implemented with the MAC/GMC software package, developed by the NASA Glenn Research Center (Ref. 37). The MAC/GMC software was utilized to perform two levels of micromechanical analysis. First, the effective properties of MD unit cells (Fig. 3) were determined. These effective properties were then used in a GMC RUC, which contained additional subcells of pure epoxy to arrive at the desired GNP volume fractions. The homogenized properties of the GNP/epoxy RUC were integrated over all possible orientations in 3-D space to simulate a random distribution of the GNPs in the epoxy matrix. Second, the corresponding properties of the randomly distributed GNP/epoxy composites were used in a subsequent MAC/GMC analysis to simulate a GNP/carbon fiber/epoxy hybrid composite. The details of these analyses are described in the following subsections.

2.2.1 GNP/Epoxy Composite

As shown on the left side of Figure 10, the GNP/epoxy was initially modeled as a GMC RUC containing the effective properties of a single MD unit cell embedded in a pure epoxy matrix. It is important to note that the MD simulations were not directly integrated into the MAC/GMC simulations. Figure 10 shows the MD simulation cell in the GMC RUC for conceptual clarity. The properties of the subcell

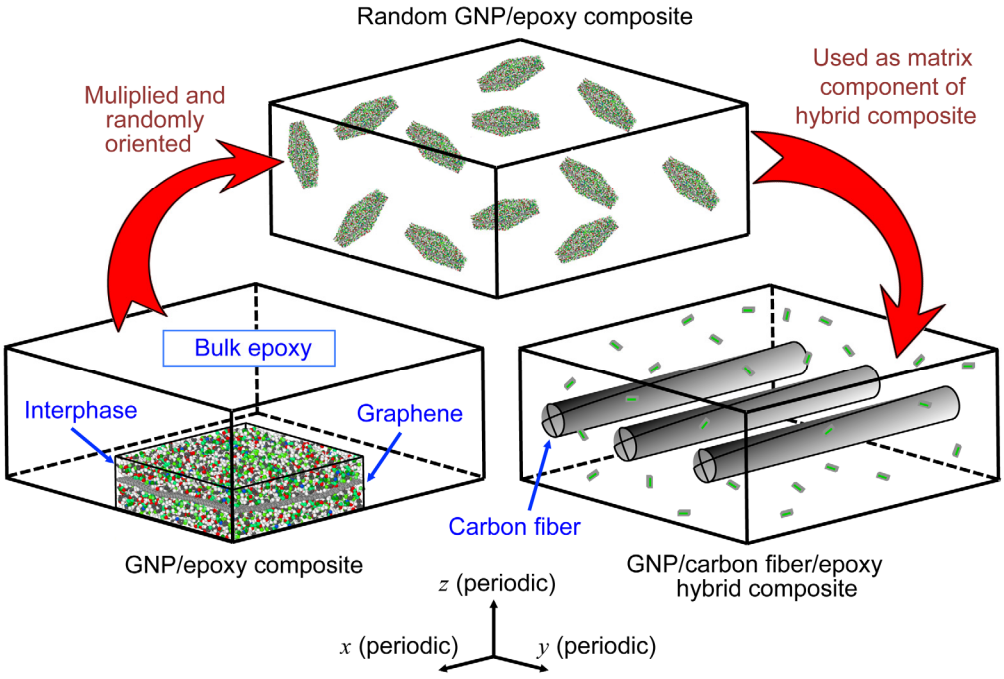

Figure 10.—Multiscale modeling scheme.

representing the MD unit were taken from Table 1, and the Young's modulus of the EPON 862/DETDA was 2.72 GPa (Ref. 3). Since the G_{xz} and G_{yz} values were nearly zero, they were given a nominal value of 1 MPa for all systems in the MAC/GMC analysis. Also, for simplicity, the values of E_x and E_y were given the same value as input in the MAC/GMC analysis for each system. The values of E_x and E_y that were input were the average values of the two quantities for each system (Table 1).

The MD models contained four different numbers of graphene sheets (1-4), each with a different volume fraction of GNP (v_{GNP} from Table 1). Thus, to obtain a specific value of GNP volume fraction for the GNP/epoxy composite in the MAC/GMC analysis, the volume of the subcell using the GNP/epoxy properties from the MD models had to be adjusted relative to the volume of the pure epoxy subcells in the RUC. Specifically, the overall GNP volume fraction in the composite (F_{GNP}) is simply the product of the volume fraction of the GNP/epoxy subcell (F_{MD}) in the MAC/GMC analysis and the volume fraction of GNP in the MD model (v_{GNP} from Table 1). That is,

$$F_{GNP} = F_{MD} v_{GNP} \tag{1}$$

Therefore, the elastic properties of the GNP/epoxy composite could be easily determined for any volume fraction of GNP without requiring new MD simulations. This approach allowed for an efficient process to predict the influence of GNP volume fraction on overall elastic properties, as detailed below.

GNP/epoxy composites typically are processed with a random distribution of GNPs within the surrounding epoxy (Fig. 10, center). To obtain the effective properties of a GNP/epoxy composite containing a random distribution of GNPs, the homogenized properties of the RUC (Fig. 10, left) were integrated over all possible orientations in 3-D space (Ref. 38). The corresponding elastic properties were thus isotropic and dependent on the GNP volume fraction and number of adjacent graphene layers together. Thus, perfect dispersion was simulated for the case of a single graphene layer, with incrementally worsening of dispersion conditions with increasing numbers of simulated layers (2-, 3-, and 4-layers). The elastic properties predicted from these simulations were used as input into the next level of MAC/GMC analysis containing the nanoenhanced epoxy matrix and carbon fibers.

2.2.2 GNP/Carbon Fiber/Epoxy Hybrid Composite

The MAC/GMC software was used to predict the elastic properties of the GNP/carbon fiber/epoxy hybrid composite shown on the right side of Figure 10. The fiber architecture was chosen as a 26 by 26 circular array shown in Figure 11. This figure shows the representative unit cell (RUC) used for composite data calculations. The outer portion (green) represents the GNP-doped epoxy, the properties of which were obtained a priori (see Section 2.2.1). The blue subcells in the center of the RUC represent the circular carbon fiber. Input parameters for the carbon fiber were chosen to accurately represent the fibers used in the experiments described below (Ref. 39), and are given in Table 2.

Figure 12 shows the predicted axial modulus of the hybrid composite as a function of GNP volume fraction for a carbon fiber volume fraction of 58 percent. From this figure it is clear that the case of perfect dispersion (1 GNP layer) results in a tensile modulus that increases at a faster rate (with respect to GNP volume fraction) than the 2-, 3-, and 4-layer scenarios. Thus, increasing levels of dispersion result in more efficient load transfer between epoxy and GNPs. However, examination of the vertical scale in Figure 12 reveals that increasing volume fractions of GNP do not result in substantial increases of axial modulus, even for the case of perfect GNP dispersion. This is because the carbon fibers dominate the reinforcing effect in the axial direction, which overshadows the contribution from the GNPs.

Figure 13 shows the predicted transverse modulus of the unidirectional hybrid composite as a function of GNP volume fraction for a fiber volume fraction of 58 percent. Similar to the results for the axial modulus (Fig. 12), the data shows the greatest reinforcing effect for the case of perfect GNP dispersion. Contrary to the results for axial modulus, the inclusion of GNPs in the hybrid composite shows a significant increase in the transverse modulus, even in the cases of 2-, 3-, and 4-layer GNPs. This result makes sense given that carbon fibers typically have a low transverse stiffness and limited influence on the transverse modulus of unidirectional composites.

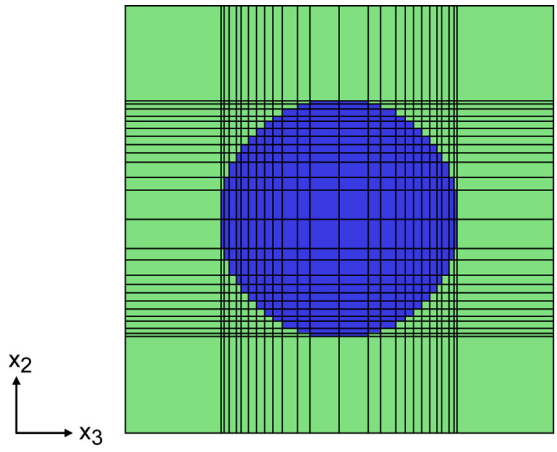

Figure 11.—MAC/GMC repeat unit cell for the GNP/carbon fiber/epoxy hybrid composite (ARCHID = 13).

TABLE 2.—MECHANICAL PROPERTIES FOR AS4 CARBON FIBERS

Property	Value
Axial modulus	231 GPa
Transverse modulus	9.6 GPa
Shear modulus	112 GPa
Poisson's ratio	0.3
Fiber volume fraction	58 percent

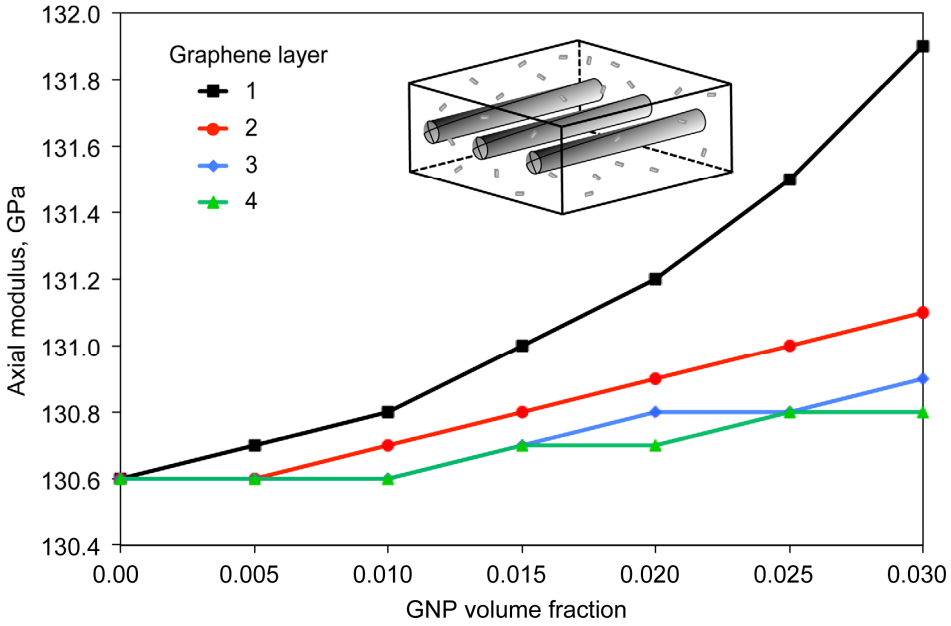

Figure 12.—Predicted axial modulus for GNP/carbon fiber/epoxy hybrid composite for varying GNP volume fraction and GNP layers.

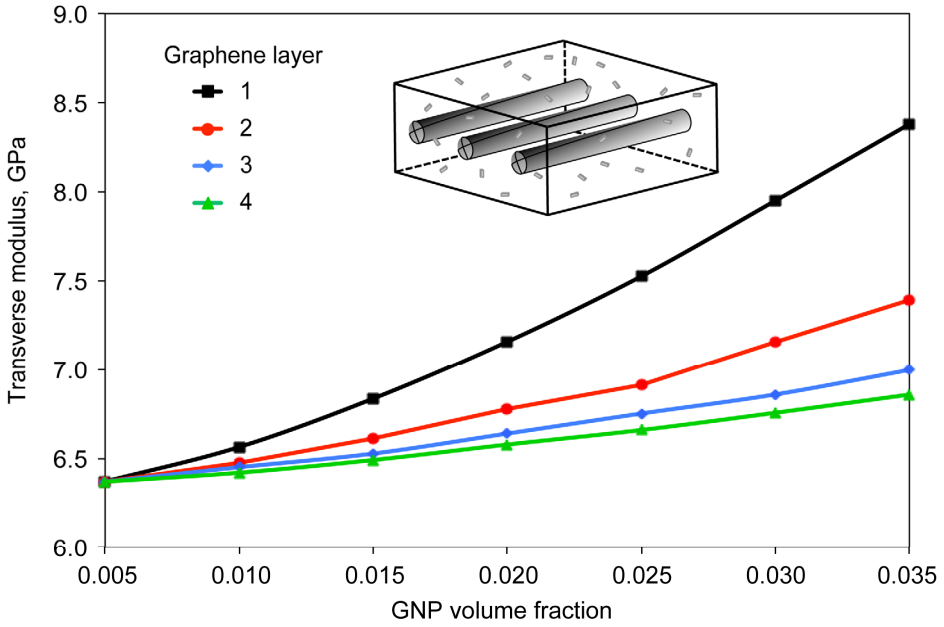

Figure 13.—Predicted transverse modulus for GNP/carbon fiber/epoxy hybrid composite for varying GNP volume fractions and GNP layers.

3.0 Experimental Fabrication and Testing

The multiscale modeling approach discussed in Section 2.0 was validated experimentally with the fabrication and mechanical testing of the GNP/carbon fiber/epoxy hybrid composite. The details of the experimental portion of this work are detailed in this section.

3.1 Materials

The epoxy material system used in this study is the same as that modeled (EPON 862/DETDA). The viscosity of EPON 862 and EPIKURE Curing Agent W at 25 °C is ~35 P and ~200 cP, respectively. EPON 862 is a low viscosity, liquid epoxy resin manufactured from epichlorohydrin and Bisphenol-F (Refs. 40 and 41). This epoxy system is available from Momentive Specialty Chemicals, Inc. The GNP system was xGnP-C-300, available from XG Sciences. It has a 2 μm average platelet diameter and a thickness of 2 nm. xGnP-C-300 has a density of ~2.0 g/ml and a surface area of 300 m^2/g (Ref. 42). Photomicrographs of xGnP are shown elsewhere (Refs. 42 to 46). The continuous carbon fiber used in this study was HexTow AS4-GP/3K (1.00 percent)(5000). HexTow AS4 carbon fiber is a continuous PAN-based fiber with a high strength and high strain, manufactured by Hexcel. The fiber was surface treated and sized (1 wt% sizing). The density of the AS4 carbon fiber is 1.79 g/mL and the modulus is 231 GPa (Ref. 39).

The concentrations (shown in wt% and the corresponding vol%) for composites tested in this study are shown in Table 3. It is important to note that increasing filler amount typically increases composite melt viscosity and, at some point, becomes difficult to fabricate into a composite part. Thus, a maximum of 3 wt% GNP was used. Table 3 also shows tensile properties determined by macroscopic methods. The results shown in Table 3 for the neat epoxy and GNP/epoxy composites have been previously reported (Refs. 3 to 47).

TABLE 3.—EXPERIMENTALLY-OBTAINED PROPERTIES FOR GNP/CARBON FIBER/ EPOXY SYSTEMS

Material system	Filler, wt%	Filler, vol%	Axial modulus, GPa
Neat epoxy	0	0.0	2.72±0.04 n = 6
GNP/epoxy	1	0.60	2.80±0.04 n = 7
GNP/epoxy	2	1.21	2.88±0.07 n = 8
GNP/epoxy	3	1.82	2.93±0.09 n = 8
Carbon fiber/epoxy	67	57.6	134.3±9.27 n = 6
GNP/carbon fiber/epoxy	GNP-0 CF-67	GNP-0 CF-58	134.29±9.27 n = 6
GNP/carbon fiber/epoxy	GNP-1 CF-67	GNP-0.8 CF-58	137.5±9.33 n = 15
GNP/carbon fiber/epoxy	GNP-2 CF-67	GNP-1.6 CF-58	137.0±6.53 n = 15
GNP/carbon fiber/epoxy	GNP-3 CF-67	GNP-2.3 CF-58	137.1±9.75 n = 11

3.2 Test Specimen Fabrication

To fabricate the neat epoxy, 100 g of EPON 862 was added to 26.4 g of EPIKURE Curing Agent W at 23 °C and mixed by hand for 3 min. The mixture was degassed inside an oven at 90 °C and 29 in. Hg vacuum for 30 min and then poured into rectangular molds. The molds were heated in an oven to 121 °C over 30 min, held at 121 °C for 2 h, heated to 177 °C over 30 min, held for another 2 h at 177 °C, and finally cooled to ambient temperature (Refs. 40, 48, and 49).

To produce the GNP/epoxy composites, the appropriate amount of GNP was added to EPIKURE Curing Agent W and mixed using a 2 in. diameter disperser blade in a Ross high shear mixer HSM-100 LSK-I at 3500 rpm for 150 min. The mixture was then placed in a Branson Bath Sonicator CPX2800H operating at 40 kHz for 60 min at 23 °C. The appropriate amount of EPON 862 was added to the GNP/Curing Agent W mixture and stirred with the Ross mixer at 1000 rpm for 3 min at 23 °C. The mixture was degassed inside an oven at 90 °C and 29 in. Hg vacuum for 30 min and then poured into rectangular-molds. The same curing cycle was used as described for the neat epoxy. For the neat epoxy and the GNP/epoxy systems, the fabricated samples were rectangular bars (165 mm long by 19 mm wide by 3.3 mm thick).

To fabricate the continuous unidirectional carbon fiber/epoxy composites, 100 g of EPON 862 was added to 26.4 g of EPIKURE Curing Agent W at 23 °C and mixed by hand for 3 min. The appropriate amount of epoxy was added to the carbon fiber tow via a winding process to produce a unidirectional composite containing 67 wt% carbon fiber and 33 wt% epoxy. The uncured epoxy/carbon fiber was cut into sheets (248 by 248 mm) and placed in a picture frame mold (254 mm by 254 in.). To fabricate the unidirectional composite plate, five plies were placed with the carbon fiber in the 0° direction. A Wabash Compression Molding Machine Vantage Series Model V75H-18-CLX was used. Initially, the composite plate was heated to 121 °C and held at a constant pressure of 30 psi for 2 hr. The press was then ramped up to 177 °C and held at a constant pressure of 1000 psi for 2 hr. Cooling water was used to cool the press until the platen temperature was 30 °C, then the composite plate (1.7 mm thick) was removed.

To fabricate the GNP/carbon fiber/epoxy hybrid composites, the appropriate amount of GNP was added to 26.4 g EPIKURE Curing Agent W and mixed using a 2 in. diameter disperser blade in a Ross high shear mixer HSM-100 LSK-I at 3500 rpm for 150 min. Next the mixture was placed in a Branson Sonicator CPX2800H operating at 40 kHz for 60 min at 23 °C. The appropriate amount of epoxy (100 g EPON 862 added to 26.4 g of EPIKURE Curing Agent W) was added to the GNP/Curing Agent W mixture and stirred with the Ross mixer at 1000 rpm for 3 min at 23 °C. The appropriate amount of GNP/epoxy were added to the carbon fiber tow using a winding process to produce a unidirectional carbon fiber composite containing the following compositions:

- 1 wt% GNP/67 wt% carbon fiber/32 wt% epoxy
- 2 wt% GNP/67 wt% carbon fiber/31 wt% epoxy
- 3 wt% GNP/67 wt% carbon fiber/30 wt% epoxy

The uncured GNP/carbon fiber/epoxy composite was cut into sheets and cured as described for the neat epoxy.

3.3 Field Emission Electron Microscope Imaging

To image the GNP in the epoxy sample at a relatively high magnification, samples were prepared for field emission electron microscopy (FESEM). Thin strips, approximately 2 mm thick by 2 mm wide by 10 mm long were cut so that the transverse tensile fracture surface would be viewed. The samples were sputtered with platinum (2 nm thickness) using an Anatech Ltd. Hummer 6.2 Sputtering System. A Hitachi S-4700 FE-SEM at 2.0 kV accelerating voltage was used to view the composites. Figure 14 shows the transverse tensile fracture surface of a 2 wt% GNP/68 wt% carbon fiber/30 wt% epoxy composite. This figure clearly shows the GNP on top of a carbon fiber.

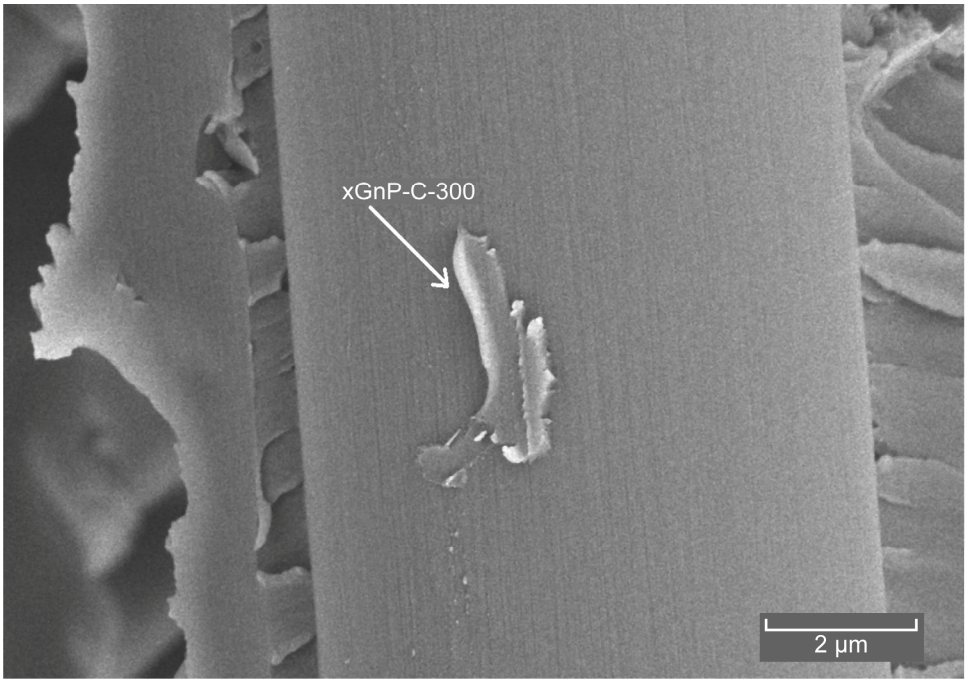

Figure 14.—FESEM image of the fracture surface of a GNP/carbon fiber/epoxy composite.

3.4 Tensile Testing

For the neat epoxy and GNP/epoxy composites, a Tensilkut Engineering router was used. The tensile properties (at ambient conditions, 16.5 cm long, 3.3 mm thick ASTM Type I sample geometry) were determined using ASTM D638 at a crosshead rate of 1 mm/min for reinforced plastics (Ref. 50). An Instru-Met Sintech screw driven mechanical testing machine was used. The tensile modulus was calculated from the initial linear portion of the stress-strain curve. For each formulation, at least 6 samples were tested. Prior to testing, the samples were conditioned at 23 °C and 50 percent relative humidity for 2 days, which is a standard ambient condition.

For the carbon fiber/epoxy and GNP/carbon fiber/epoxy composites, tensile bars were cut to 12.7 mm wide and a length of 203 mm. Tabbing material (fiberglass/epoxy) was attached to the ends of each sample. The tensile properties were determined using ASTM D3039 at a crosshead rate of 2 mm/min for fiber reinforced plastics (Ref. 51). The same mechanical testing machine and conditioning was used as described in the previous paragraph.

Table 3 shows the tensile results (mean, standard deviation, and number of samples tested) for the neat epoxy, GNP/epoxy composites, carbon fiber/epoxy, and GNP/carbon fiber/epoxy composites. From the data it is clear that adding 1 to 3 wt% GNP to carbon fiber/epoxy composites did not cause the axial modulus to change significantly. This result is expected due to the large amount and high axial modulus of the carbon fiber.

4.0 Discussion

This section will discuss the combined computational/experimental results. First, the combined results for the GNP/epoxy materials will be covered, followed by the results for the GNP/carbon fiber/epoxy hybrid composite.

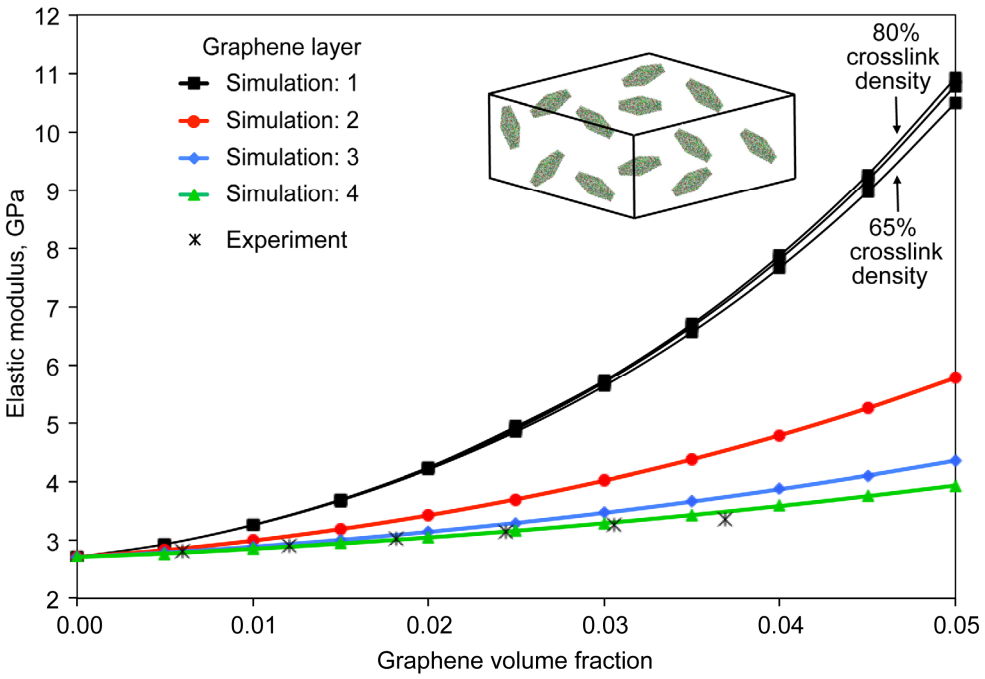

Figure 15.—Elastic modulus of GNP/epoxy composite for both computational and experimental approaches.

4.1 GNP/Epoxy Composite

Figure 15 shows the combined computational/experimental results for the elastic modulus of GNP/epoxy system for 1-4 layers of graphene. There are three important observations from this Figure. First, it is clear that increases in GNP volume fraction have a significant effect on the elastic modulus in the case of perfect dispersion. For lower levels of dispersion, the influence of GNP on the elastic modulus is greatly diminished. Second, the figure shows excellent agreement between the experimental data and the 4-layer GNP/epoxy model, suggesting that the computational model is valid and that the experimental specimens have, on average, at least 4 GNP layers adhered together. This observation reveals that the multiscale model is a powerful tool that can be used to assess the dispersion quality in GNP-reinforced polymers. Finally, the data in Figure 15 also indicate that the epoxy crosslink density (shown only for the 1-layer system for clarity) has a minimal effect on the elastic modulus of the GNP/epoxy composite for the crosslink density range considered.

4.2 GNP/Carbon Fiber/Epoxy Hybrid Composite

Figure 16 shows the experimentally determined and computationally predicted axial modulus of the GNP/carbon fiber/epoxy composite as a function of GNP volume fraction. This figure shows the same computational data shown in Figure 12 with the experimental data given in Table 3. There are several important points of discussion concerning this figure. First, the agreement between the models and experiment validates the multiscale modeling method. However, there are some discrepancies between the predictions and the experimental data for the carbon fiber/GNP/epoxy systems. This could indicate some error in the properties used for the carbon fiber in the models, or variation in the volume fraction of the carbon fiber. Second, the predicted increase in axial modulus is insignificant relative to the experimental scatter associated with the experiments (error bars for the experimental data points indicates standard deviation from replicate tests). Third, the data indicate that the influence of GNPs on the hybrid composite axial modulus is minimal, regardless of the GNP volume fraction. Since the carbon fiber dominates the stiffness in the axial direction, it is not practical to use nanoenhanced epoxy to improve the

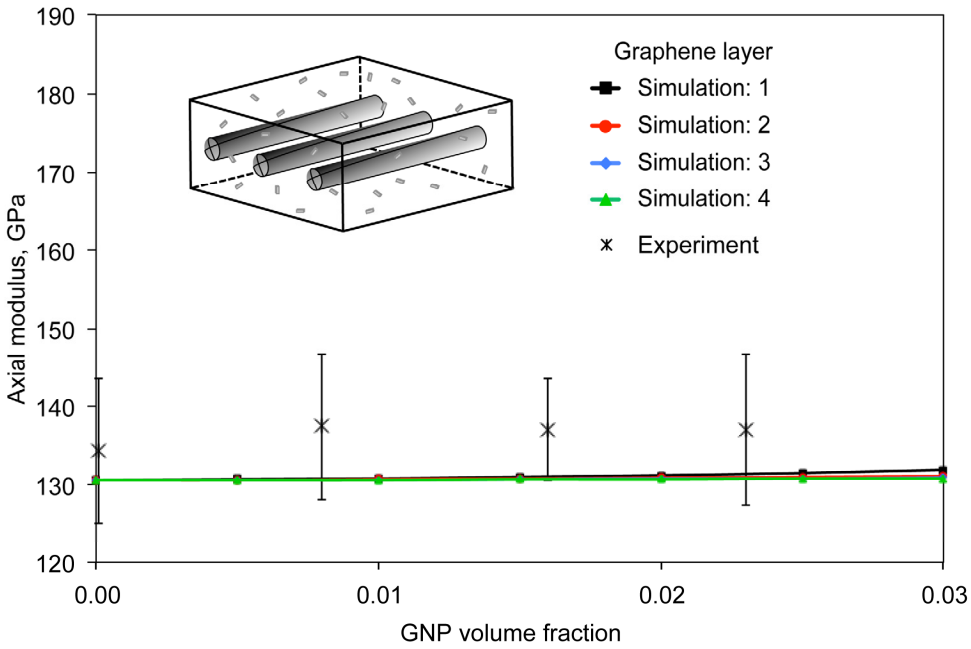

Figure 16.—Axial elastic modulus of GNP/carbon fiber/epoxy composite for both computational and experimental approaches.

axial stiffness. However, doping the epoxy matrix of a carbon fiber/epoxy system with GNP can provide significant transverse and shear reinforcement and improve the performance of the structure in the event that it encounters unexpected loads. Moreover, the use of GNP may allow for the minimization of the transverse and shear reinforcing plies in the structural design, reducing the overall weight of the structure. Finally, the epoxy crosslink density (for the crosslink density range considered herein) has a negligible influence on the axial modulus.

5.0 Conclusions

In this study a hierarchical multiscale modeling method has been developed and experimentally validated to predict the elastic properties of GNP/epoxy composites and GNP/carbon fiber/epoxy hybrid composites. The multiscale modeling method incorporates MD simulation on the molecular level and micromechanical simulation on the microscopic level. Fabrication and testing of specimens of the modeled materials were used to validate the model and to provide insight into the capabilities of the modeling method.

There are four major conclusions from this research. First, the developed multiscale modeling method is accurate and can provide physical insight into the mechanical behavior of GNP-reinforced composites. This includes the potential to use the method to quantify GNP dispersion via correlation of simulation and test data. Second, the GNP volume fraction in the hybrid composite can have a strong influence the composite transverse tensile and shear properties. Third, GNP dispersion quality has a strong effect on the transverse tensile and shear properties of the composite. Fourth, GNP volume fraction and dispersion has a minimal influence on the hybrid composite axial properties where the carbon fiber is the primary reinforcement agent. Therefore, GNP-doping in carbon fiber/epoxy composites is most valuable in cases where composite parts are designed to transmit significant loads in the direction transverse to the fiber alignment or protect the structure against unforeseen loading scenarios.

References

1. Kuilla T, Bhadra S, Yao DH, Kim NH, Bose S, Lee JH. Recent advances in graphene based polymer composites. Prog Polym Sci. 2010;35(11):1350-1375.
2. Rafiee MA, Rafiee J, Wang Z, Song HH, Yu ZZ, Koratkar N. Enhanced Mechanical Properties of Nanocomposites at Low Graphene Content. ACS Nano. 2009;3(12):3884-3890.
3. King JA, Klimek DR, Miskioglu I, Odegard GM. Mechanical properties of graphene nanoplatelet/epoxy composites. J Appl Polym Sci. 2013;128(6):4217-4223.
4. Tang LC, Wan YJ, Yan D, Pei YB, Zhao L, Li YB, et al. The effect of graphene dispersion on the mechanical properties of graphene/epoxy composites. Carbon. 2013;60:16-27.
5. Hadden CM, Jensen BD, Bandyopadhyay A, Odegard GM, Koo A, Liang R. Molecular modeling of EPON-862/graphite composites: Interfacial characteristics for multiple crosslink densities. Compos Sci Technol. 2013;76:92-99.
6. Bandyopadhyay A, Valavala PK, Clancy TC, Wise KE, Odegard GM. Molecular modeling of crosslinked epoxy polymers: The effect of crosslink density on thermomechanical properties. Polymer. 2011;52(11):2445-2452.
7. Varshney V, Patnaik S, Roy A, Farmer B. A Molecular Dynamics Study of Epoxy Based Networks: Cross-linking Procedure and Prediction of Molecular and Material Properties. Macromolecules. 2008;41(18):6837-6842.
8. Fan HB, Yuen MMF. Material properties of the cross-linked epoxy resin compound predicted by molecular dynamics simulation. Polymer. 2007;48(7):2174-2178.
9. Li CY, Strachan A. Molecular dynamics predictions of thermal and mechanical properties of thermoset polymer EPON862/DETDA. Polymer. 2011;52(13):2920-2928.
10. Frankland SJV, Caglar A, Brenner DW, Griebel M. Molecular Simulation of the Influence of Chemical Cross-Links on the Shear Strength of Carbon Nanotube-Polymer Interfaces. J Phys Chem B. 2002;106(12):3046-3048.
11. Odegard GM, Gates TS, Wise KE, Park C, Siochi EJ. Constitutive modeling of nanotube-reinforced polymer composites. Compos Sci Technol. 2003;63(11):1671-1687.
12. Frankland SJV, Harik VM, Odegard GM, Brenner DW, Gates TS. The stress-strain behavior of polymer-nanotube composites from molecular dynamics simulation. Compos Sci Technol. 2003;63(11):1655-1661.
13. Clancy TC, Gates TS. Modeling of interfacial modification effects on thermal conductivity of carbon nanotube composites. Polymer. 2006;47(16):5990-5996.
14. Zhu R, Pan E, Roy AK. Molecular dynamics study of the stress-strain behavior of carbon-nanotube reinforced Epon 862 composites. Mat Sci Eng a-Struct. 2007;447(1-2):51-57.
15. Nouranian S, Jang C, Lacy TE, Gwaltney SR, Toghiani H, Pittman CU. Molecular dynamics simulations of vinyl ester resin monomer interactions with a pristine vapor-grown carbon nanofiber and their implications for composite interphase formation. Carbon. 2011;49(10):3219-3232.
16. Gou JH, Minaie B, Wang B, Liang ZY, Zhang C. Computational and experimental study of interfacial bonding of single-walled nanotube reinforced composites. Comput Mater Sci. 2004;31 (3-4):225-236.
17. Ionita M. Multiscale molecular modeling of SWCNTs/epoxy resin composites mechanical behaviour. Compos Part B-Eng. 2012;43(8):3491-3496.
18. Odegard GM, Clancy TC, Gates TS. Modeling of the mechanical properties of nanoparticle/polymer composites. Polymer. 2005;46(2):553-562.
19. Yu S, Yang S, Cho M. Multi-scale modeling of cross-linked epoxy nanocomposites. Polymer. 2009;50(3):945-952.
20. Jang C, Lacy TE, Gwaltney SR, Toghiani H, Pittman CU. Interfacial shear strength of cured vinyl ester resin-graphite nanoplatelet from molecular dynamics simulations. Polymer. 2013;54(13): 3282-3289.

21. Stevens MJ. Interfacial fracture between highly cross-linked polymer networks and a solid surface: Effect of interfacial bond density. Macromolecules. 2001;34(8):2710-2718.
22. Mansfield KF, Theodorou DN. Atomistic Simulation of a Glassy Polymer Graphite Interface. Macromolecules. 1991;24(15):4295-4309.
23. Gao JS, Shiu SC, Tsai JL. Mechanical properties of polymer near graphite sheet. J Compos Mater. 2013;47(4):449-458.
24. Li CY, Browning AR, Christensen S, Strachan A. Atomistic simulations on multilayer graphene reinforced epoxy composites. Compos Pt A-Appl Sci Manuf. 2012;43(8):1293-1300.
25. Plimpton S. Fast Parallel Algorithms for Short-Range Molecular-Dynamics J Comput Phys. 1995;117(1):1-19.
26. Jorgensen WL, Maxwell DS, Tirado-Rives J. Development and Testing of the OPLS All-Atom Force Field on Conformational Energetics and Properties of Organic Liquids. J Am Chem Soc. 1996;117:11225-11236.
27. Watkins EK, Jorgensen WL. Perfluoroalkanes: Conformational analysis and liquid-state properties from ab initio and Monte Carlo calculations. J Phys Chem A. 2001;105(16):4118-4125.
28. Hoover WG. Canonical Dynamics - Equilibrium Phase-Space Distributions. Phys Rev A. 1985;31(3):1695-1697.
29. Varley RJ, Heath GR, Hawthorne DG, Hodgkin JH, Simon GP. Toughening of a Trifunctional Epoxy System .1. Near-Infrared Spectroscopy Study of Homopolymer Cure. Polymer. 1995;36(7):1347-1355.
30. Wang Q, Storm BK, Houmoller LP. Study of the isothermal curing of an epoxy prepreg by near-infrared spectroscopy. J Appl Polym Sci. 2003;87(14):2295-2305.
31. Musto P, Martuscelli E, Ragosta G, Russo P. The curing process and moisture transport in a tetrafunctional epoxy resin as investigated by FT-NIR spectroscopy. High Perform Polym. 2000;12(1):155-168.
32. Dannenberg H. Determination of Functional Groups in Epoxy Resins by Near-Infrared Spectroscopy. SPE Transactions. 1963;3(1):78-88.
33. George GA, Coleclarke P, Stjohn N, Friend G. Real-Time Monitoring of the Cure Reaction of a Tgddm/Dds Epoxy-Resin Using Fiber Optic Ft-Ir. J Appl Polym Sci. 1991;42(3):643-657.
34. Paley M, Aboudi J. Micromechanical Analysis of Composites by the Generalized Cells Model. Mech Mater. 1992;14(2):127-139.
35. Bednarcyk BA, Aboudi J, Arnold SM. The effect of general statistical fiber misalignment on predicted damage initiation in composites. Compos Part B-Eng. 2014;66:97-108.
36. Aboudi J, Arnold SM, Bednarcyk BA. Micromechanics of Composite Materials: A Generalized Multiscale Analysis Approach: Elsevier, Inc.; 2013.
37. Bednarcyk BA, Arnold SM. MAC/GMC user's manual - keywords manual. NASA/TM 2002-212077/Vol 2. 2002.
38. Christensen RM, Waals FM. Effective Stiffness of Randomly Oiriented Fiber Composites. J Compos Mater. 1972;6:518-535.
39. Hexcel. HexTow Continuous Carbon Fiber Product Literature. Stamford, CT, 2011.
40. Momentive Specialty Chemicals. EPON 862/EPIKURE Curing Agent W System Product Literature. 180 E. Broad Street, Columbus, OH, 2011.
41. Tack JL, Ford DM. Thermodynamic and mechanical properties of epoxy resin DGEBF crosslinked with DETDA by molecular dynamics. J Mol Graph Model. 2008;26(8):1269-1275.
42. XG Sciences. xGnP Brand Graphene Nanoplatelets Product Information. 3101 Grand Oak Drive, Lansing, MI, 2010.
43. Kalaitzidou K, Fukushima H, Drzal LT. Mechanical properties and morphological characterization of exfoliated graphite-polypropylene nanocomposites. Compos Pt A-Appl Sci Manuf. 2007;38(7):1675-1682.
44. Fukushima H, T Drzal L, Rook BP, Rich MJ. Thermal conductivity of exfoliated graphite nanocomposites. J Therm Anal Calorim. 2006;85(1):235-238.

45. Kalaitzidou K, Fukushima H, Miyagawa H, Drzal LT. Flexural and tensile moduli of polypropylene nanocomposites and comparison of expermental data to Halpin-Tsai and Tandon-Wang models. Polym Eng Sci. 2007;47(11):1796-1803.
46. Kalaitzidou K, Fukushima H, Drzal LT. A new compounding method for exfoliated graphite-polypropylene nanocomposites with enhanced flexural properties and lower percolation threshold. Compos Sci Technol. 2007;67(10):2045-2051.
47. King JA, Klimek DR, Miskioglu I, Odegard GM. Mechanical Properties of Grahene Nanoplatelet/Epoxy Composites. J Compos Mater. 2014;In press.
48. Zhou YX, Pervin F, Lewis L, Jeelani S. Fabrication and characterization of carbon/epoxy composites mixed with multi-walled carbon nanotubes. Mat Sci Eng a-Struct. 2008;475(1-2):157-165.
49. Chen CG, Curliss D. Processing and morphological development of montmorillonite epoxy nanocomposites. Nanotechnology. 2003;14(6):643-648.
50. American Society for Testing and Materials. ASTM D638 Standard Test Method for Tensile Properties of Polymer Matrix Composite Materials. Philadelphia, PA2008.
51. American Society for Testing and Materials. ASTM D3039 Standard Test Method for Tensile Properties of Polymer Matrix Composite Materials. Philadelphia, PA2008.